Reductive and Oxidative Half-Reactions of Morphinone Reductase from *Pseudomonas putida* M10: A Kinetic and Thermodynamic Analysis†

Daniel H. Craig,‡ Peter C. E. Moody,‡ Neil C. Bruce,§ and Nigel S. Scrutton*,‡

Department of Biochemistry, University of Leicester, Adrian Building, University Road, Leicester LE1 7RH U.K., and Institute of Biotechnology, University of Cambridge, Tennis Court Road, Cambridge CB2 1TP

Received February 12, 1998; Revised Manuscript Received March 16, 1998

ABSTRACT: The reaction of morphinone reductase (MR) with the physiological reductant NADH and the oxidizing substrate codeinone has been studied by multiple and single wavelength stopped-flow spectroscopy. Reduction of the enzyme with NADH proceeds in two kinetically resolvable steps. In the first step, the oxidized enzyme forms a charge-transfer intermediate with NADH. The charge-transfer complex is characterized by an increase in absorbance at long wavelength (540 to 650 nm), and its rate of formation is dependent on substrate concentration and is controlled by a second-order rate constant of 4.8×10^5 M^{-1} s^{-1} at pH 7.0 and 5 °C. In the second step, the enzyme-bound flavin is reduced to the dihydroflavin form. The rate of flavin reduction (23.4 s^{-1} at pH 7.0 and 5 °C) is independent of substrate concentration and is observed as a monophasic decrease in absorbance at 462 nm. The oxidative half-reaction proceeds in three kinetically resolvable steps. The first is due to the formation of a reduced enzyme−codeinone charge-transfer complex and is observed at long wavelength (about 650 nm). The rate of charge-transfer complex formation is dependent on codeinone concentration and is controlled by a second-order rate constant of 11.5×10^3 M^{-1} s^{-1} at pH 7.0 and 5 °C. The second step represents flavin reoxidation and is observed at 462 (absorption increase) and 650 nm (absorption decrease) and progresses with a rate (about 45 s^{-1}) which is independent of codeinone concentration. The third step is observed as a further small increase in absorbance at 462 nm and proceeds with a rate of about 2.5 s^{-1}. This step most likely represents hydrocodone release from the oxidized enzyme. Analysis of the temperature dependence of the reductive half-reaction has enabled calculation of the entropic and enthalpic contributions for charge-transfer formation, charge-transfer decay (yielding free enzyme and substrate), and electron transfer to the enzyme-bound FMN, and the construction of a partial energy profile for the reaction catalyzed by MR. The reaction scheme and redox properties of MR are compared with those described previously for the closely related flavoprotein, old yellow enzyme. Although common features are identified, there are notable differences in the kinetic and redox properties of the two enzymes.

Morphinone reductase (MR)[1] from *Pseudomonas putida* M10 catalyzes the NADH-dependent saturation of the carbon−carbon double bond of morphinone and codeinone, yielding hydromorphone and hydrocodone, respectively. Together with morphine dehydrogenase, MR catalyzes the first step in the degradation of morphine and codeine [Figure 1, (*1*)]. Both enzymes are potentially useful for the production of semisynthetic opiate drugs. Given the widespread use of hydromorphone as a powerful analgesic [seven times more potent than morphine (*2*)] and of hydrocodone as a mild antitussive (*3*), the use of specific biocatalysts to produce these compounds is an attractive alternative to the traditional methods of synthesis (*4*). The difficulty associated with specifically oxidizing the C-6 hydroxy group of morphine has previously compromised chemical approaches to the synthesis of hydromorphone; while thebaine, the starting material for the synthesis of hydrocodone, is often in limiting supply. To enable biological synthesis of hydromorphone and hydrocodone, the genes encoding morphine dehydrogenase and morphinone reductase have been cloned and expressed in *Escherichia coli* to provide, on the industrial scale, recombinant strains capable of converting morphine and codeine into hydromorphone and hydrocodone, respectively (*5*, *6*).

MR is a homodimeric flavoprotein of M_r 82 200 containing one molar equivalent of noncovalently bound FMN per enzyme subunit (*7*). Sequence analysis of the gene (*mor* B) encoding MR has identified the enzyme as a member of the growing family of Class I flavin-dependent β/α barrel oxidoreductases (*7*, *8*); other members of the family include the isoforms of old yellow enzyme [OYE (*9*)], pentaerythritol tetranitrate, and glycerol trinitrate reductases (*10*, *11*), an oestrogen-binding protein (*12*), several expressed sequence tags from plants [see ref 7 and references therein] and the

† This work was funded by grants from the Biotechnology and Biological Sciences Research Council (NSS, PCEM, NCB) and the Royal Society (NSS).

* To whom correspondence should be addressed. Tel: +44 116 223 1337. Fax: +44 116 252 3369. E-mail: nss4@le.ac.uk.

‡ University of Leicester.

§ University of Cambridge.

[1] Abbreviations: MR, morphinone reductase; OYE, old yellow enzyme; FMN, flavin mononucleotide.

S0006-2960(98)00345-6 CCC: $15.00
Published on Web 04/30/1998

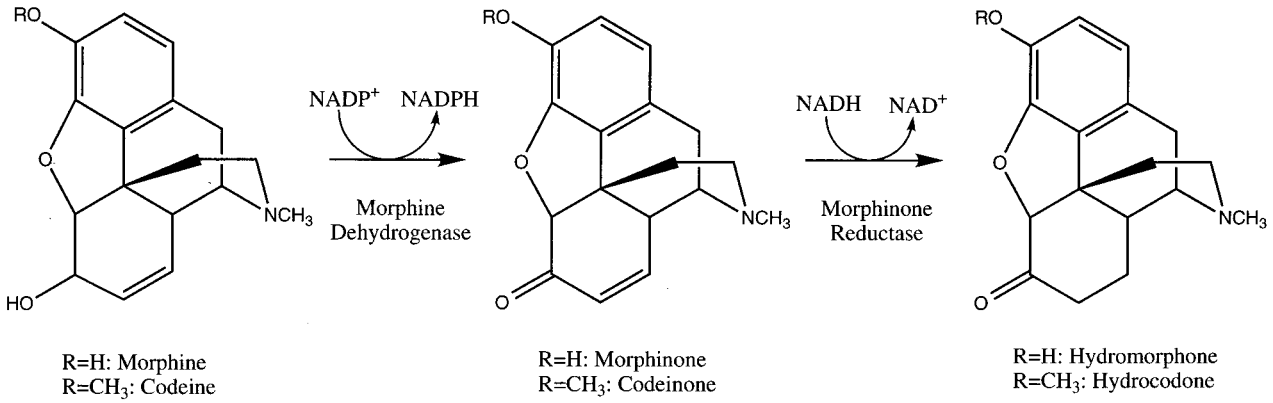

FIGURE 1: The reactions catalyzed by morphine dehydrogenase and morphinone reductase. Morphine dehydrogenase catalyzes the oxidation of the C6 hydroxy group of morphine to form morphinone, and morphinone reductase reduces the 7,8-olefinic bond of morphinone to yield hydromorphone.

more complex enzymes tri- and dimethylamine dehydrogenase (*13*, *14*), *Thermoanaerobium brockii* NADH oxidase (*15*), and the bile acid inducible proteins *bai* H and *bai* C from *Eubacterium* sp VPI12708 (*11*, *17*). MR has been crystallized (*18*) and the structure of the enzyme has been solved at 2.5 Å resolution (Moody et al., unpublished). The crystallographic structure has revealed a homodimer of subunits, each folded as an 8-fold β/α barrel, typical of the Class I flavin-dependent β/α barrel oxidoreductases (*8*, *19*). Although the subunit structure and mode of FMN binding in MR are similar to those reported for OYE (*20*), the interactions responsible for subunit assembly are completely different (Moody et al., unpublished).

The reaction catalyzed by MR is of the hybrid two-site double displacement type (*21*), and the binding sites for NADH and codeinone are located on the *si* face of the flavin isoalloxazine ring. The reaction sequence comprises two half-reactions viz reduction of the flavin by NADH (the reductive half-reaction) producing NAD^+ and the dihydroflavin form of the enzyme-bound FMN, and reoxidation of the reduced flavin by morphinone or codeinone (the oxidative half-reaction) to yield hydromorphone or hydrocodone (*21*). MR shares many properties with OYE and estrogen-binding protein; each enzyme is inhibited by the steroids cortisone and progesterone, and each is able to reduce the unsaturated carbon−carbon bond of cyclohexen-1-one. These common catalytic properties support a common evolutionary origin inferred by comparison of the gene sequences encoding the enzymes (*7*).

In this paper, we have examined the kinetic behavior of MR using multiple and single wavelength stopped-flow methods. The kinetic data are used to identify intermediates in the reaction sequence catalyzed by MR and to derive microscopic rate constants for their interconversion. By using temperature-dependent studies, we have also derived thermodynamic parameters for some steps in the reaction sequence enabling the construction of a partial energy profile for the reaction catalyzed by MR. The data provide a detailed kinetic and thermodynamic framework for the reaction catalyzed by the enzyme. Parallels are seen with the reaction catalyzed by the homologous OYE of *Saccharomyces* sp, but notable differences in the redox and kinetic behavior are also observed.

EXPERIMENTAL PROCEDURES

Chemicals and Enzymes. Complex bacteriological media were from Unipath and all media were prepared as described by Sambrook et al. (*22*). α- and β-NADH, glucose oxidase, and lactate dehydrogenase were purchased from Sigma. Codeinone was kindly supplied by Dr. M. McPherson (MacFarlan Smith Ltd, Edinburgh, UK) and Timentin was from Beecham Research Laboratories. Morphinone reductase was purified from an overexpressing strain of *E. coli* as described previously (*21*), except that Timentin was substituted for Ampicillin during the growth of the overexpressing strain. Enzyme for kinetic work was contained in 50 mM potassium phosphate buffer, pH 7.0 and 2 mM 2-mercaptoethanol. Enzyme subunit concentrations were determined from the 462 nm absorbance of oxidized enzyme using an extinction coefficient of 11 300 M^{-1} cm^{-1} in 50 mM potassium phosphate buffer, pH 7.0. 5-Deazaflavin mononucleotide was a kind gift of Professor S. Ghisla (University of Konstanz). The concentration of NADH was determined spectrophotometrically using an extinction coefficient of 6 220 M^{-1} cm^{-1}.

Photoreduction of MR. Photoreduction of MR was essentially as described for other flavoproteins (*23*), but modified to utilize the catalytic effects of 5-deazaflavin mononucleotide (*24*, *25*). Enzyme (1.5 mL), contained in 50 mM potassium phosphate buffer, pH 7.0, was mixed with 0.5 units of glucose oxidase in a cuvette attached to a glass tonometer with sidearm. A solution (0.4 mL) of β-D-glucose and EDTA, pH 8.0 was added to the sidearm so that, on mixing with the enzyme solution, the final β-D-glucose and EDTA concentrations were 15 and 67 mM, respectively. The tonometer was made anaerobic by repeated evacuation and flushing with argon gas made oxygen-free by passing through an oxygen-scrubbing catalyst (Peak Scientific Ltd). Following the establishment of anaerobic conditions, the sidearm contents were mixed with the enzyme and illuminated at 4 °C with a 60 W reflector bulb held at a distance of 15 cm from the cuvette. Spectra were recorded using a Hewlett-Packard 8452A single-beam diode array spectrophotometer. Following reduction of the enzyme, air was admitted to the tonometer to enable reoxidation of the enzyme-bound flavin.

Kinetic Measurements. Rapid reaction kinetic experiments were performed using an Applied Photophysics SF.17MV stopped-flow spectrophotometer. For reactions performed

under anaerobic conditions, the stopped-flow apparatus was positioned within a customized anaerobic glovebox (Belle Technology Ltd). An oxygen-free environment was maintained by purging the glovebox with nitrogen gas and by circulating the gas through a BASF catalyst R3-11. The stopped-flow circuitry was left standing overnight in dithionite solution and flushed thoroughly with anaerobic buffer prior to reaction analysis. Solutions were prepared for anaerobic work by evacuation and placement in the glovebox for 2 h prior to use.

Time-dependent reductions of MR with NADH were perfomed by multiple wavelength stopped-flow spectroscopy using a photodiode array detector and X-SCAN software (Applied Photophysics). Spectral deconvolution was perfomed by global analysis and numerical integration methods using PROKIN software (Applied Photophysics). For single-wavelength studies, data collected at 462, 550, and 650 nm were analyzed using nonlinear least-squares regression analysis on an Archimedes 410-1 microcomputer using Spectrakinetics software (Applied Photophysics). Experiments were performed by mixing MR in the appropriate buffer with an equal volume of NADH in the same buffer at the desired concentration. For studies of the oxidative half-reaction, the sequential mixing mode of the stopped-flow apparatus was used. Enzyme was rapidly mixed with a stoichiometric amount of NADH to enable reduction of the enzyme-bound flavin and after a suitable aging period (see below), codeinone was then rapidly mixed with the reduced enzyme solution and reoxidation monitored at 462 or 650 nm. The intrinsic oxidase activity of MR was found to be sufficiently slow to enable the use of sequential mixing protocols for analysis of the oxidative half-reaction with codeinone, but not cyclohexene-1-one, as substrate (see below). In reductive and oxidative reactions, the concentration of substrate was always at least 10-fold greater than that of MR, thereby ensuring pseudo-first-order conditions. For each substrate concentration, at least five replica measurements were collected and averaged.

Observed rate constants for flavin absorption changes at 462 nm following mixing with NADH were obtained from fits of the data to eq 1

$$A_{462} = Ce^{-k_{obs1}t} + b \quad (1)$$

where C is a constant related to the initial absorbance and b is an offset value to account for a nonzero baseline. Transients at 462 nm for the oxidative half-reaction were fit to eq 2 that describes a double exponential process

$$A_{462} = C_1(1 - e^{-k_{obs1}t}) + C_2(1 - e^{-k_{obs2}t}) + b \quad (2)$$

where k_{obs1} and k_{obs2} are the observed rate constants for the faster and slower phases, respectively, and C_1 and C_2 are related to the initial absorbance. b is an offset, again to account for a nonzero baseline. In the reductive half-reaction, transients at 552 nm were fitted to eq 3

$$A_{552} = k_{obs1}C\frac{e^{-k_{obs1}t} - e^{-k_{obs2}t}}{k_{obs2} - k_{obs1}} + b \quad (3)$$

where C is a constant related to the initial absorbance, b is an offset, k_{obs1} is the observed rate constant for the increase in absorbance at 552 nm (charge-transfer formation), and k_{obs2} is the observed rate constant for the decrease in absorbance at 552 nm (flavin reduction). For the oxidative half-reaction, transients at 650 nm were also fit to eq 3, where k_{obs1} is the observed rate constant for charge-transfer formation (i.e., reduced enzyme−codeinone complex) and k_{obs2} is the observed rate constant for charge-transfer decay. For the reductive and oxidative half-reaction, the "up" phase (k_{obs1}; charge-transfer formation) of the 552 and 650 nm transients, respectively, was found to depend linearly on NADH or codeinone concentration, respectively, and data were fitted to eq 4

$$k_{obs1} = k_1[S] + k_{-1} \quad (4)$$

where k_1 is the second-order rate constant for the formation of the charge-transfer complex, and k_{-1} is the first-order rate constant for the decay of the charge-transfer complex to form free enzyme and substrate. The "down" phase at 552 and 650 nm (k_{obs2}; charge-transfer decay) was found to be independent of substrate concentration (except at low substrate concentrations for the oxidative half-reaction where kinetic mixing effects yield a small apparent dependency; see Results).

The reductive half-reaction sequence was modeled as shown in the general scheme

$$A + B \underset{k_{-1}}{\overset{k_1}{\rightleftharpoons}} C \underset{k_{-2}}{\overset{k_2}{\rightleftharpoons}} D \quad (5)$$

where A = MR_{ox}, B = NADH, C = MR−NADH charge-transfer complex, and D = MR containing the dihydroflavin form of the FMN (with bound NAD^+); although NAD^+ release occurs following enzyme reduction, spectral signatures for NAD^+ release were not identified and this step is not incorporated in the kinetic scheme. For the oxidative half-reaction, the reaction sequence was modeled as shown in the general scheme

$$A + B \underset{k_{-1}}{\overset{k_1}{\rightleftharpoons}} C \xrightarrow{k_2} D \xrightarrow{k_3} E + F \quad (6)$$

where A = two electron-reduced MR, B = codeinone, C = reduced MR−codeinone charge-transfer complex, D = MR_{ox} with bound hydrocodone, E = MR_{ox}, and F = hydrocodone. All curve fitting was performed using the Grafit software package (*26*).

RESULTS

Photoreduction of MR. Light-mediated reduction of MR using 5-deazaflavin mononucleotide as catalyst proceeded slowly and complete reduction was obtained only following prolonged exposure (>6 h). Inclusion of the soluble mediator benzyl viologen during the course of photoreduction accelerated the rate of photoreduction (complete within 1 h exposure). The spectral changes accompanying photoreduction contrast markedly with those seen for the highly related OYE (*25*). Photoreduction of OYE proceeds in a two-step mechanism, initially producing the red anionic semiquinone, with its characteristic spectral peak at about 380 nm, before further reduction produces the two-electron reduced dihydroflavin form of the enzyme-bound flavin. During photoreduction of MR, spectral changes characteristic

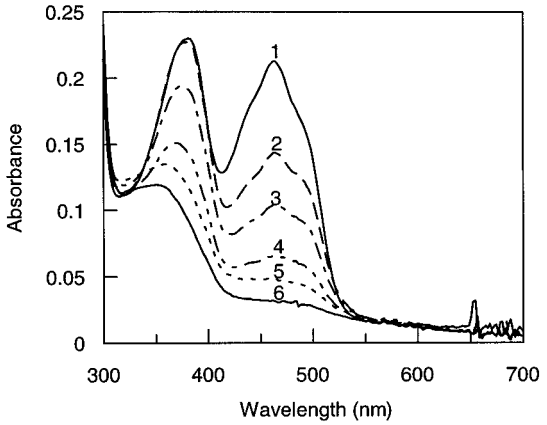

FIGURE 2: Photoreduction of MR. Conditions: 20 μM MR, 15 mM β-D-glucose, 67 mM EDTA, 0.5 units glucose oxidase, 50 mM potassium phosphate buffer, pH 7.0. Curve 1, before illumination; curves 2−6, after 17, 60, 135, 265, and 365 min illumination. After irradiation, air was admitted and the original spectrum was regained rapidly.

of the red anionic semiquinone or the blue neutral semiquinone were not observed, and the enzyme-bound flavin was converted directly to the dihydroflavin form (Figure 2). Following the admission of oxygen to the tonometer, the reduced enzyme was converted directly to the oxidized and fully active form of the enzyme; semiquinone formation was not seen during the conversion of the two electron-reduced enzyme to the oxidized enzyme. The flavin environment in MR, unlike that in OYE, is probably not suitable for the stabilization of the red anionic semiquinone, and future structural comparisons of the two enzymes may reveal the nature of this difference in redox behavior. However, if there is an appreciable dismutation reaction of any potential semiquinone form, it remains a possibility that the slow rate of reduction of MR may prevent the observation of semiquinone formation. In this regard, it is noteworthy that, unlike MR, complete reduction of OYE is achieved relatively quickly (about 12 min) using photoreduction methods (*25*).

Multiple and Single Wavelength Stopped-Flow Studies of the Reductive Half-Reaction. Analysis of the spectral changes seen in the course of the reaction of MR with NADH was performed by rapid-mixing photodiode array spectroscopy. Reduction of the enzyme with β-NADH at pH 7.0 (five times molar excess of NADH) revealed the existence of three enzyme species. Kinetic data were analyzed globally by numerical integration using a three-state model

$$A \rightarrow B \rightarrow C$$

where A = oxidized enzyme, B = an enzyme−NADH charge-transfer intermediate and, C = enzyme containing the dihydroflavin form of FMN. The enzyme−NADH charge-transfer complex gives rise to an absorbance increase at long wavelength (540 to 650 nm) and a small decrease in the absorbance of the flavin at 460 nm (Figure 3). However, the spectral form of the flavin in the charge-transfer state clearly indicates that the enzyme is in the oxidized form (Figure 3). The spectral form of species C is consistent with electron transfer having occurred from NADH to the enzyme-bound FMN. Reduction of the flavin was not complete indicating some back reaction (and see below), that is, conversion of species D to C in eq 5. Complete reduction

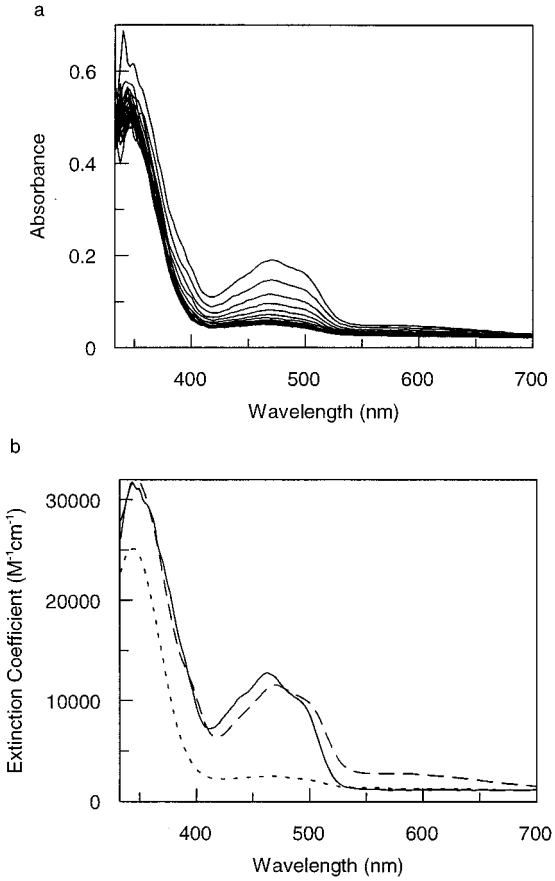

FIGURE 3: Spectral changes occurring in the reductive half-reaction of MR. Panel a, time-dependent spectral changes for MR mixed with NADH. The first spectrum was recorded 1.28 ms after mixing. Conditions: 20 μM MR, 100 μM NADH, 50 mM potassium phosphate buffer, pH 7.0, 5 °C. Panel b, deconvoluted spectra of initial, intermediate, and final forms of the enzyme obtained by global analysis using ProKin software. Spectrum 1 (solid line), oxidized enzyme; spectrum 2 (hatched line), charge-transfer intermediate; spectrum 3 (dotted line), two electron-reduced enzyme.

of the flavin was only obtained when relatively high concentrations of NADH [>20-fold molar excess over the concentration of MR (20 μM)] were used in stopped-flow experiments. Stopped-flow experiments performed with and without NADH as substrate clearly indicated that spectral changes did not occur during the dead time (1 ms) of the stopped-flow apparatus, thus indicating, unlike for OYE, that an additional enzyme−NADH intermediate is not observed for MR prior to the formation of the charge-transfer intermediate. Also, in contrast to OYE, α-NADH was found not to be a substrate for MR, since no spectral changes were observed on mixing α-NADH with MR.[2]

The spectral changes observed in the multiple wavelength studies revealed that 552 nm is a convenient wavelength for monitoring the formation and decay of the enzyme−NADH charge-transfer complex (Figure 4). The large absorption changes at 462 nm are appropriate for monitoring the electron-transfer step (C → D of eq 5; Figure 4). The rate of change of absorbance at 462 nm (flavin reduction) is

[2] Prior to stopped-flow experiments, α-NADH was incubated with pyruvate and lactate dehydrogenase to remove any contamination with β-NADH. Stopped-flow reactions were performed over a range of α-NADH concentrations extending from 24 to 445 μM.

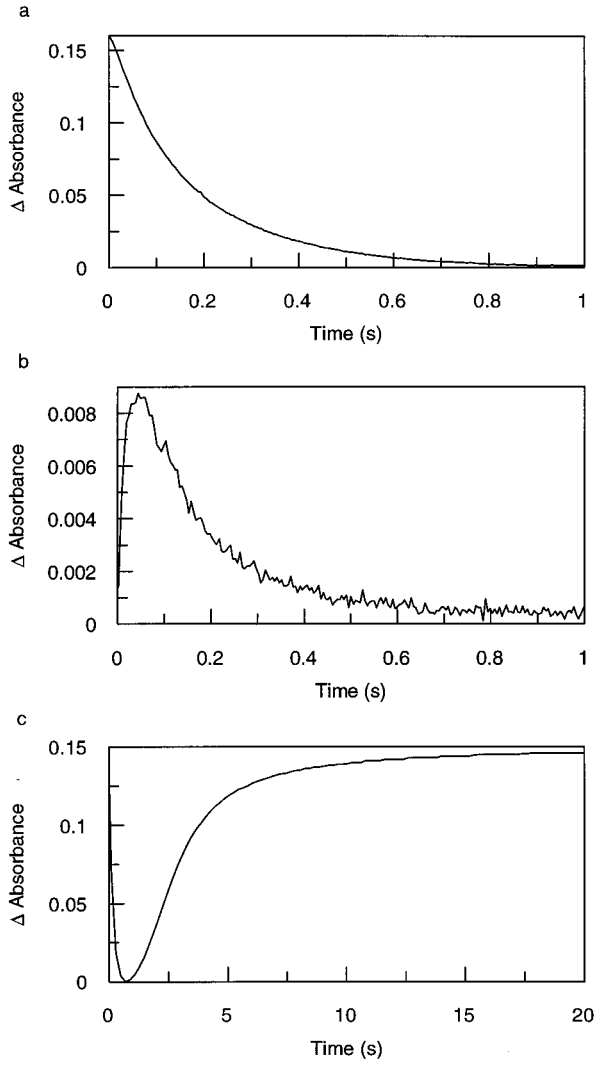

FIGURE 4: Kinetic transients observed for the reductive half-reaction of MR. Panel a, transient observed at 462 nm; panel b, transient observed at 552 nm; panel c, transient observed at 462 nm over an extended time base, illustrating the reoxidation of the enzyme-bound FMN by molecular oxygen. Conditions: 20 μM MR, 20 μM NADH contained in 50 mM potassium phosphate buffer, pH 7.0; reactions performed at 5 °C.

identical to the rate calculated for the down phase of the transient recorded at 552 nm (decay of the charge-transfer intermediate), indicating that decay of the charge-transfer complex is a direct consequence of flavin reduction. Charge-transfer formation is not readily observed at 462 nm since both steps of the reductive half-reaction sequence give rise to a decrease in absorbance at this wavelength and the magnitude of the absorbance change for formation of the charge-transfer intermediate is small compared with the flavin reduction step. In contrast, however, the "up−down" nature of the kinetic transient at 552 nm (Figure 4) makes calculation of the rates for charge-transfer formation and decay a relatively simple process. When reactions were performed aerobically with stoichiometric concentrations of NADH and enzyme over extended periods of time, the transients displayed "down−up" behavior at 462 nm, indicating that the enzyme-bound flavin is reoxidized by molecular oxygen (Figure 4). Under anaerobic conditions the "up" phase is lost and the enzyme remains in the two electron-reduced dihydroflavin form. Full spectrum analysis under

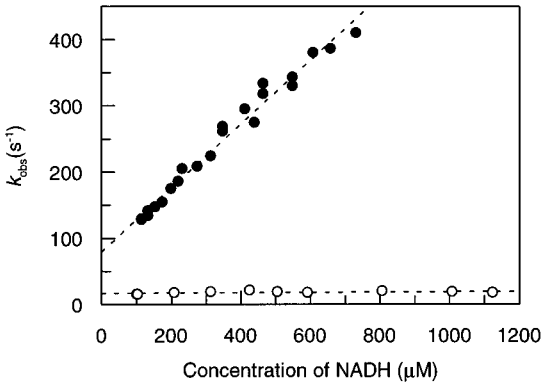

FIGURE 5: Concentration dependence of the observed rate constants measured at 552 (charge-transfer formation and decay) and 462 nm (electron transfer). Conditions: 20 μM MR, 50 mM potassium phosphate buffer, pH 7.0, 5 °C.

anaerobic conditions using a stoichiometric concentration or a five times molar excess of NADH also revealed that flavin reduction was not complete. The data are therefore consistent with there being an appreciable reverse reaction for the flavin reduction step.

Kinetic and Thermodynamic Analysis of the Reductive Half-Reaction. The observed rate constant (k_{obs1}) for formation of the charge-transfer complex exhibited a linear dependence with respect to NADH concentration (Figure 5). Least-squares fitting to eq 4 provided a second-order rate constant for charge-transfer formation of 4.8×10^5 M^{-1} s^{-1} and a first-order rate constant (ordinate intercept) of 80 s^{-1} for decay of the charge-transfer complex to yield free enzyme and NADH (at pH 7.0 and 5 °C). The dissociation constant for the charge-transfer complex is 166 μM [compared with an apparent K_m for NADH of 50 μM measured in the steady state in the same buffer at 30 °C and with 0.3 mM codeinone (*21*)]. In contrast, the observed rate constant for flavin reduction was found to be independent of NADH concentration, consistent with the proposed reaction scheme (eq 5). Rate constants for flavin reduction (k_2) and the formation and decay of the charge-transfer complex (k_1 and k_{-1}) were calculated for data collected over the temperature range 5−23 °C (Table 1; Figure 5). Rate constants were then analyzed using the Arrhenius equation, written in terms of transition-state theory (eq 7)

$$k = \frac{k_B}{h} T e^{-\Delta G^{\ddagger}/RT} = \frac{k_B}{h} T e^{-\Delta H^{\ddagger}/RT} e^{\Delta S^{\ddagger}/R} \qquad (7)$$

where k_B is Boltzmann's constant and h is Planck's constant. Data were fitted to eq 8, and values of $\Delta S^{\ddagger}$ and $\Delta H^{\ddagger}$ were calculated from the values of the ordinate intercept and gradient, respectively (Figure 6).

$$R\left[\ln\left(\frac{k}{T}\right) - \ln\left(\frac{k_B}{h}\right)\right] = \Delta S^{\ddagger} - \Delta H^{\ddagger}\left(\frac{1}{T}\right) \qquad (8)$$

The errors in the calculated value of $\Delta S^{\ddagger}$ will be larger than those associated with $\Delta H^{\ddagger}$ due to the large extrapolation to the ordinate axis. However, conclusions drawn from temperature-dependence studies of the reductive half-reaction, which rely on the sign and magnitude of $\Delta S^{\ddagger}$, are not likely to be compromised. The validity of performing an extrapolation to the ordinate axis to calculate values of ΔS

Table 1: Temperature Dependence of Rate and Dissociation Constants for the Reductive Half-Reaction of MR

Formation and Decay of Charge-Transfer Intermediate

temperature (K)	k_1 (M^{-1} s^{-1})	k_{-1} (s^{-1})	K_d (μM)
278.0	$4.8 \times 10^5 \pm 0.1 \times 10^5$	80.0 ± 6.1	166 ± 16.1
280.4	$5.6 \times 10^5 \pm 0.2 \times 10^5$	98.0 ± 8.7	175 ± 21.9
282.7	$7.1 \times 10^5 \pm 0.1 \times 10^5$	89.6 ± 5.2	126 ± 9.1
285.3	$7.9 \times 10^5 \pm 0.4 \times 10^5$	130.6 ± 14.2	165 ± 26.3
287.7	$9.4 \times 10^5 \pm 0.2 \times 10^5$	148.1 ± 7.6	158 ± 11.5
291.7	$10.6 \times 10^5 \pm 0.3 \times 10^5$	170.7 ± 11.6	161 ± 15.5
295.9	$12.1 \times 10^5 \pm 0.9 \times 10^5$	218.6 ± 24.5	180.7 ± 33.7

Electron Transfer from NADH to Enzyme-Bound FMN

temperature (K)	k_2 (s^{-1})	temperature (K)	k_2 (s^{-1})
277.6	23.4 ± 0.1	298.1	52.4 ± 0.1
280.7	25.5 ± 0.05	298.2	52.9 ± 0.1
283.7	27.5 ± 0.05	300.6	58.4 ± 0.1
285.7	29.2 ± 0.1	303.1	63.5 ± 0.2
288.7	33.8 ± 0.1	304.0	65.0 ± 0.2
290.7	36.8 ± 0.1	307.0	69.8 ± 0.2
292.7	39.7 ± 0.1	310.4	75.1 ± 0.2
295.4	46.1 ± 0.1		

was recently demonstrated in studies of oligonucleotide binding to the *Tetrahymena* group I ribozyme (*27*); even after making conservative estimates for the errors in the relevant kinetic and binding constants, the errors in ΔS were found not to compromise conclusions concerning the entropy-driven binding to the ribozyme's oligonucleotide substrate. In the above example, variations in rate constants of up to 2-fold and dissociation constants by ±50% were seen between experiments. In our studies of MR, the values of the observed rates used to calculate the thermodynamic parameters varied by no more than about ±1%, thereby ensuring, by comparison to the work of Narlikar and Herschlag (*27*), a relatively small error in the $\Delta S^{\ddagger}$ value.

Analysis of the rates for the concentration-independent electron-transfer step (k_2) by eq 8 revealed a large negative entropy change ($\Delta S^{\ddagger} = -125.9 \pm 2.7$ J mol^{-1} K^{-1}) on forming the transition state. This more ordered transtion state probably reflects charge formation during electron transfer, since positive charge is developed on the nicotinamide and negative charge develops in the N1/C2 carbonyl region of the flavin isoalloxazine ring. Development of these charged species will lead to ordering of solvent molecules in the active site. The enthalpic contribution ($\Delta H^{\ddagger}$) to the electron-transfer step is 25.7 ± 0.8 kJ mol^{-1}, and the corresponding change in Gibbs free energy ($\Delta G^{\ddagger}$), calculated at 298 K, is 63.2 ± 1.6 kJ mol^{-1}. In contrast to the electron-transfer step, formation of the charge-transfer intermediate from free enzyme and β-NADH is associated with a weakly negative entropy change ($\Delta S^{\ddagger} = -16.2 \pm 11.6$ J mol^{-1} K^{-1}), an enthalpic contribution ($\Delta H^{\ddagger}$) of 33.0 ± 3.2 kJ mol^{-1}, and a change in Gibbs free energy ($\Delta G^{\ddagger}$) of 37.8 ± 6.7 kJ mol^{-1} (calculated at 298 K). Clearly, the small negative change in entropy is the result of contributions made by the immobilization of NADH in the active site (ordering), desolvation of the active site (disordering), and possibly reversible changes in conformation on binding NADH leading to a more "open" structure in the transition state (disordering). Whether formation of the transition state is associated with a "loosening" of structure remains to be shown. In this regard, it is worth noting that crystals of MR can be reduced by the addition of NADH contained in mother liquor. Following enzyme reduction in the crystalline form, the crystals remain intact and preliminary structural analysis of the reduced enzyme indicates that major structural changes do not occur on reduction with NADH (Moody et al., unpublished). These findings argue against major conformational changes as the transition state forms, but more subtle structural changes may be tolerated in the crystalline form of MR. Decay of the charge-transfer complex to form free enzyme and NADH is associated with values for $\Delta S^{\ddagger}$, $\Delta H^{\ddagger}$, and $\Delta G^{\ddagger}$ of -76.9 ± 13.4 J mol^{-1} K^{-1}, 36.4 ± 3.8 kJ mol^{-1} and 59.34 ± 7.8 kJ mol^{-1}, respectively. As an additional verification of the accuracy of the thermodynamic figures derived by fitting data to eq 8, the Gibbs free energy change for the equilibrium relating the free enzyme/substrate forms and the charge-transfer complex can be calculated from the value of the dissociation constant for the charge-transfer complex. In this case, ΔG_{eq} at 298 K is 21.4 kJ mol^{-1}, which is almost identical to the value of 21.5 kJ mol^{-1} calculated from the difference in the Gibbs free energies ($\Delta G^{\ddagger}_{reverse} - \Delta G^{\ddagger}_{forward}$) for the transition state associated with formation and decay of the charge-transfer complex. The agreement in the two figures, therefore, underlines the accuracy of the thermodynamic parameters calculated by fitting kinetic data to eq 8.

Analysis of the Oxidative Half-Reaction by Sequential Stopped-Flow Studies. Studies of the reductive half-reaction under aerobic conditions indicated that the intrinsic oxidase activity of MR was slow (0.2 s^{-1}). Therefore, as an alternative to employing anaerobic conditions and the mixing of dithionite-reduced MR with oxidizing substrate, a sequential mixing protocol was developed to analyze the oxidative half-reaction. The method involved the rapid mixing of stoichiometric (20 μM) amounts of NADH with MR and, following an appropriate delay (700 ms) to enable reduction of the enzyme, the mixing of the oxidizing substrate with the aged reaction. Sequential mixing protocols of this type are valid only if the rates of reoxidation by the oxidizing substrate are sufficiently faster than the intrinsic oxidase rate, thereby enabling kinetic resolution. Preliminary investigations using cyclohexen-1-one as substrate revealed that MR was reoxidized at similar rates in the presence and absence of this substrate. Clearly, in this case the rate of reoxidation by cyclohexen-1-one is slower, or at best equivalent, to the intrinsic oxidase rate. In contrast, however, the rate of reoxidation by codeinone was found to be at least 100-fold greater than the rate of reoxidation by molecular oxygen, thus demonstrating that codeinone reoxidation rates could be determinined using the sequential mixing protocol.

Analysis of the spectral changes accompanying the reaction of two electron-reduced MR with codeinone at pH 7.0 by multiple wavelength photodiode array spectroscopy revealed that the oxidative half-reaction was best described by a sequential reaction scheme involving four spectral species (Figure 7)

$$A \rightarrow B \rightarrow C \rightarrow D$$

Global fitting for the above reaction scheme and deconvolution of the spectra for intermediates provided evidence for the nature of the intermediate species (Figure 7). The spectrum of species A resembles that of a mixture of MR containing predominantly the dihydroflavin form of FMN

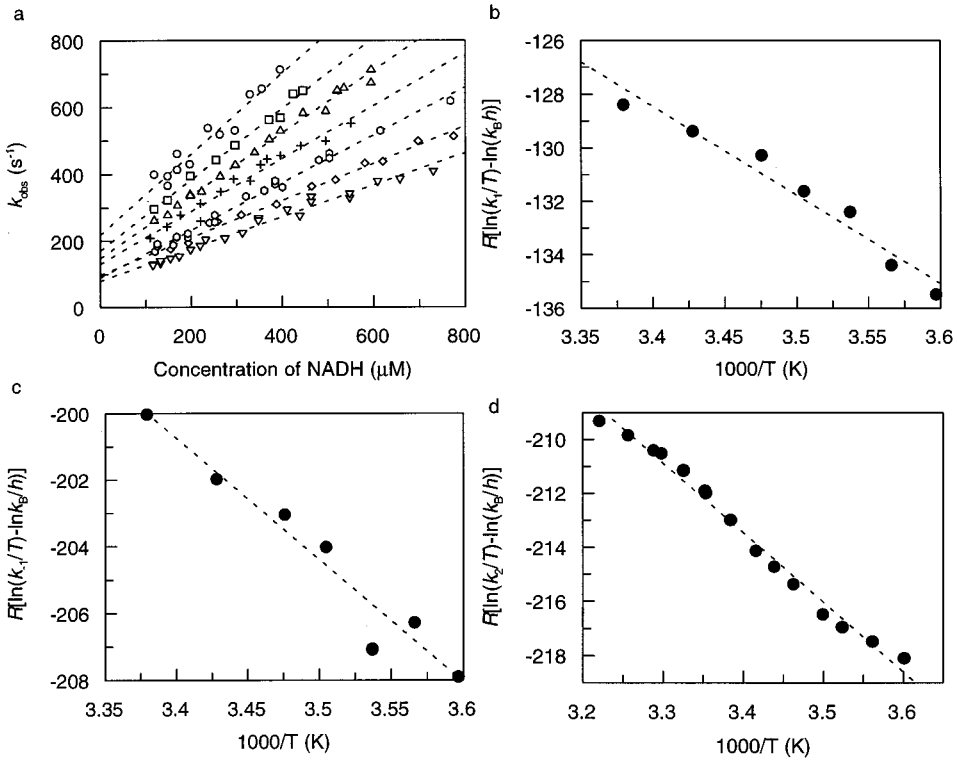

FIGURE 6: Thermodynamic analysis of the two sequential steps in the reductive half-reaction of MR. Panel a, plot of observed rate constant at 552 nm versus NADH concentration at various temperatures. Data for reactions perfomed at 5 (inverted triangles), 7.4 (diamonds), 9.7 (hexagons), 12.3 (crosses), 14.7 (triangles), 18.7 (squares), and 22.9 °C (circles) are shown. Calculated values for k_1, k_{-1}, and K_d are given in Table 1. Panel b, thermodynamic analysis of the temperature dependence of k_1: $\Delta S^{\ddagger} = -16.2 \pm 11.6$ J mol^{-1} K^{-1}, $\Delta H^{\ddagger} = 33.0 \pm 3.2$ kJ mol^{-1}, $\Delta G^{\ddagger}$ (at 298 K) $= 37.8 \pm 6.7$ kJ mol^{-1}. Panel c, thermodynamic analysis of the temperature dependence of k_{-1}: $\Delta S^{\ddagger} = -76.9 \pm 13.4$ J mol^{-1} K^{-1}, $\Delta H^{\ddagger} = 36.4 \pm 3.8$ kJ mol^{-1}, $\Delta G^{\ddagger}$ (at 298 K) $= 59.3 \pm 7.8$ kJ mol^{-1}. Panel d, thermodynamic analysis of the temperature dependence of k_2 (electron transfer). Rate constants are given in Table 1: $\Delta S^{\ddagger} = -125.9 \pm 2.7$ J mol^{-1} K^{-1}, $\Delta H^{\ddagger} = 25.7 \pm 0.8$ kJ mol^{-1}, $\Delta G^{\ddagger}$ (at 298 K) $= 63.2 \pm 1.6$ kJ mol^{-1}.

and some oxidized FMN. The mixed redox state at the start of the oxidative half-reaction arises because stoichiometric amounts of NADH were used to prereduce the enzyme; our work on the reductive half-reaction clearly demonstrated that stoichiometric amounts of NADH, and indeed a 5 times molar excess of NADH (Figure 3), are insufficient to completely reduce MR, indicating that flavin reduction is reversible. It is important to appreciate, therefore, that the deconvoluted spectra for the oxidative half-reaction are not the true spectra for the various identified intermediates because a small and constant amount of MR_{ox} is present throughout this sequence of reactions. Nevertheless, from the nature of the spectral changes it is a relatively straightforward task to assign each of the spectral changes to the presence of intermediates in the oxidative half-reaction. The spectrum of species B exhibits a broad increase in absorbance at long wavelengths and also a small increase at 462 nm. This spectrum is characteristic of a charge-transfer intermediate and represents the complex formed between two electron-reduced MR and codeinone. The spectrum of species C indicates a collapse in the long-wavelength charge-transfer band and a substantial increase in the absorbance at 462 nm. These spectral changes on forming species C are indicative of flavin reoxidation achieved by electron transfer to codeinone to yield hydrocodone. Finally, a fourth species (species D) accumulates at the end of the oxidative half-reaction which has a slightly enhanced absorbance at 462 nm. The formation of this species has been tentatively assigned to the release of hydrocodone from the oxidized enzyme.[3] The deconvoluted spectra indicate that reoxidation of MR does not pass through a semiquinone state since absorbance changes associated with the blue (neutral) or red (anionic) semiquinone forms were not observed. As expected, therefore, reoxidation is a two electron-transfer process leading to saturation of the olefinic bond in codeinone.

Further evidence to support the assignment of the various intermediates observed in the oxidative half-reaction was gained by analyzing the concentration dependence of the three kinetic phases. These analyses were performed in single-wavelength mode at 462 and 650 nm. The transients at 650 nm displayed typical "up−down" behavior reflecting formation and subsequent decay of the charge-transfer intermediate (Figure 8). At 462 nm, the transients were complex; they are strictly triphasic, but the first phase (charge-transfer formation) is difficult to observe because it occurs rapidly and its amplitude is small compared with the amplitude of the intermediate phase (flavin reoxidation). The

[3] Long-term storage (several hours) of codeinone in aqueous buffer leads to undefined chemical changes to the substrate which affect the kinetic behavior of MR. Care was taken with kinetic work to always work quickly with codeinone solutions and for aqueous solutions to be stored for very short periods of time at −70 °C. Under these conditions, the kinetic data were entirely reproducible. Also, analysis of the codeinone sample by matrix-assisted laser desorption mass spectrometry indicated a pure product, free of breakdown or modified forms. Therefore, the last kinetic phase observed in the oxidative half-reaction is unlikely to be the result of reduced MR reacting with modified forms of codeinone.

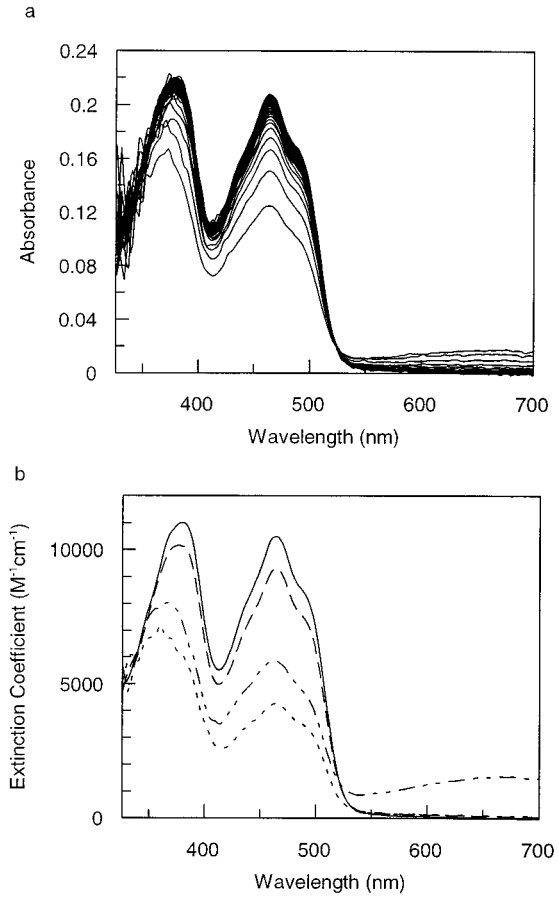

FIGURE 7: Time-dependent spectral changes for the reaction of reduced MR with codeinone. Enzyme (cell concentration 20 μM) was reduced with a stoichiometric amount of NADH, and following a delay time of 700 ms, codeinone (1 mM) was rapidly mixed with the enzyme. Conditions: 50 mM potassium phosphate buffer, pH 7.0, 5 °C. Panel a, time-dependent spectral changes for the reaction. Panel b, deconvoluted spectra obtained by fitting the data to a four-state model (see text for details) using ProKin software. Mixture of two electron-reduced (predominant form) and oxidized enzyme (lower dotted spectrum); codeinone-reduced MR charge-transfer intermediate (upper dotted spectrum); oxidized enzyme bound to hydrocodone (hatched spectrum); oxidized MR (solid spectrum).

slow phase (probably hydrocodone release from oxidized enzyme) is clearly resolved from the intermediate phase. Transients at 462 nm were fit to eq 3, after removing the very early part of the transient (charge-transfer formation) from the data (Figure 8). Although this is an approximation, the data analysis clearly revealed that the intermediate phase observed at 462 nm (flavin reoxidation) has a rate identical to the "down" phase seen at 650 nm (charge-transfer decay), thus demonstrating that these processes are kinetically equivalent. Analysis of the three kinetic steps as a function of codeinone concentration revealed that charge-transfer formation at 650 nm was dependent on codeinone concentration, and data were best fit to eq 4. The second-order rate constant for charge-transfer formation at 5 °C and pH 7 was calculated as $11.5 \pm 1.1 \times 10^3$ M^{-1} s^{-1}. The ordinate intercept revealed the existence of a reverse reaction with first-order rate constant 89.9 ± 6.3 s^{-1}. The calculated dissociation constant for the two electron-reduced MR−codeinone complex is 7.8 ± 1.4 mM. Analysis of the "down" rate at 650 nm revealed that reoxidation of the flavin was essentially independent of codeinone concentration, except at low codeinone concentrations where kinetic mixing

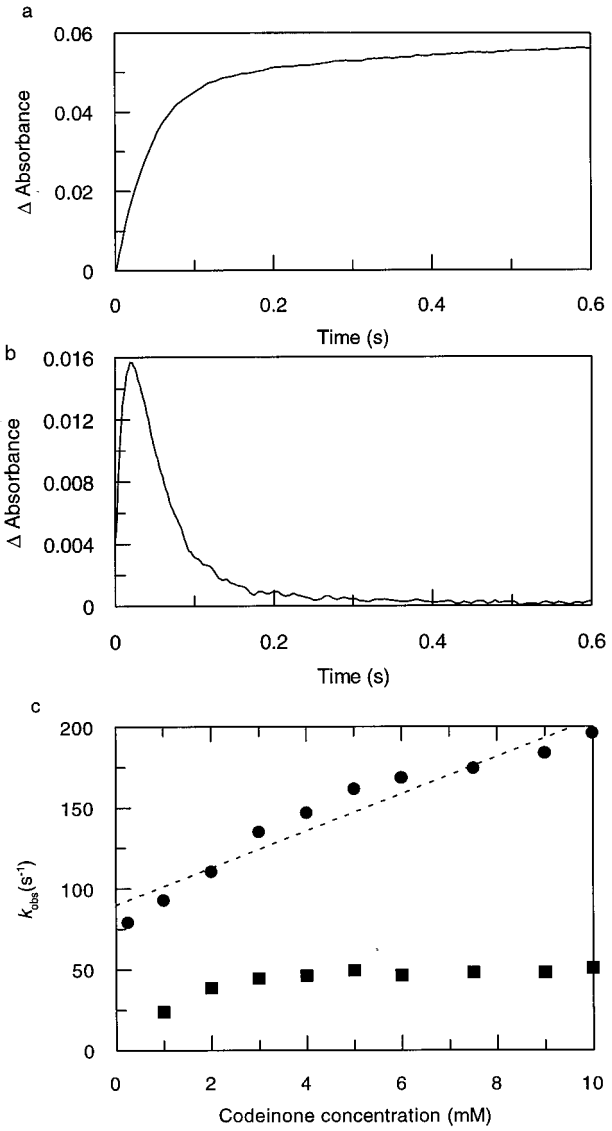

FIGURE 8: Kinetic transients observed for the oxidative half-reaction of MR and concentration dependence of the 650 nm transients. Panel a, transient observed at 462 nm; panel b, transient observed at 650 nm; panel c, concentration dependence of the observed rate constants measured at 650 [charge-transfer formation and decay (circles)] and 462 nm [flavin reoxidation (squares)]. Conditions: 20 μM MR, 20 μM NADH (both cell concentrations) contained in 50 mM potassium phosphate buffer, pH 7.0 and premixed with a delay time of 700 ms before reaction with codeinone contained in the same buffer. All reactions performed at 5 °C.

with the formation of the charge-transfer complex gives rise to an apparent dependency. Analysis of the slow phase observed at 462 nm as a function of codeinone concentration also revealed that the rate of this phase is independent of codeinone concentration (Table 2). Kinetic analysis at various pH values clearly indicated that the pseudobiphasic nature of the kinetic transients observed at 462 nm and pH 7.0 (Figure 8) was also seen at other pH values (pH range 6−9). This observation rules out the possibility that multiple forms of the enzyme (in different protonic states due to reversible ionization of an active site residue) are responsible for the observed biphasic kinetic transients. This finding therefore lends more support to the notion that the slow step at 462 nm represents product release from oxidized MR.

Further analysis of the oxidative half-reaction using the thermodynamic approach described above for the reductive

Table 2: Dependence on Codeinone Concentration of the Rate Constants for the Three Kinetically Resolvable Phases of the Oxidative Half-Reaction of MR[a]

codeinone (mM)	k_{obs1} (s^{-1})	k_{obs2} (s^{-1})	k_{obs3} (s^{-1})
0.25	78.8 ± 1.3	nd	nd
1	92.7 ± 0.9	23.8 ± 0.2	2.3 ± 0.1
2	110.3 ± 1.0	38.5 ± 0.3	3.4 ± 0.1
2.5	nd	nd	2.9 ± 0.1
3	134.9 ± 1.5	44.4 ± 0.4	nd
4	146.8 ± 1.3	46.1 ± 0.3	nd
5	161.3 ± 2.6	49.2 ± 0.7	3.8 ± 0.2
6	168.3 ± 6.7	46.2 ± 0.2	nd
7.5	174.1 ± 2.1	48.1 ± 0.4	nd
9	183.4 ± 1.0	48.1 ± 0.2	nd
10	195.9 ± 1.7	50.7 ± 0.3	2.5 ± 0.2

[a] k_{obs2} and k_{obs3} are essentially independent of substrate concentration and are therefore the true microscopic rate constants for flavin reoxidation and hydrocodone release, respectively. nd, not determined. Values for k_{obs1} and k_{obs2} were determined at 650 nm and values for k_{obs3} at 462 nm.

half-reaction was not possible due to the prohibitive amounts of codeinone required (codeinone is not commercially available). The poor stability of morphinone and also the lack of a commercial source likewise prevented analysis of the oxidative half-reaction with this opiate compound.

DISCUSSION

In this study, the kinetic mechanism of MR has been studied by stopped-flow spectroscopy using the physiological reductant NADH and the oxidizing substrate codeinone. Although the enzyme is closely related to the isoforms of OYE (*7*), major differences in the kinetic properties of the two enzymes were observed. First, during photoreduction of MR, the semiquinone form of the flavin was not observed during light-mediated reduction, indicating that the flavin environment in MR is significantly different from that in OYE; semiquinone stabilization is seen in OYE during the course of photoreduction. Second, MR was not reduced by α-NADH. This is in contrast to OYE, which has a preference for α-NADPH over *β*-NADPH in stopped-flow and steady-state turnover experiments (*28*). Reduction of the flavin in OYE by NADPH showed it to be rate-limiting in overall catalysis, but in the case of MR, the slow final kinetic phase of the oxidative half-reaction (attributed to hydrocodone release from oxidized enzyme) is much slower than flavin reduction and is therefore the most likely rate-limiting step for MR. Other differences between the two enzymes can also be discerned, for example, the lack of a discrete binding step prior to charge-transfer formation in the reductive half-reaction of MR. With OYE, such a binding step was inferred from spectral changes occurring in the dead time of the stopped-flow instrument (*28*). The oxidative half-reactions of the two enzymes also differ substantially. With MR, the reaction is more complex involving a reduced MR−codeinone charge-transfer complex, an electron transfer step, and a kinetically resolvable product release step. With OYE, the oxidative half-reaction is simplified—there being no charge-transfer formation when cyclohexen-1-one is used as substrate—and it is best described by the formation of a reduced enzyme−cyclohexen-1-one complex by a rapid equilibrium process followed by electron transfer (*28*). It remains possible, however, that reactions of MR with cyclohexen-1-one may also proceed

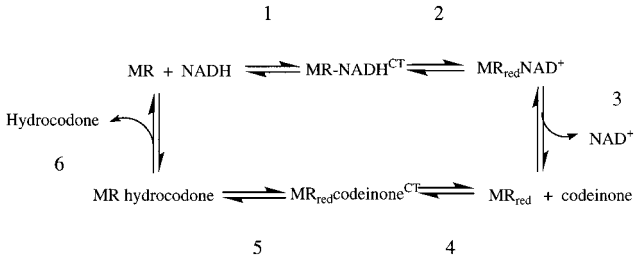

FIGURE 9: The reaction scheme catalyzed by MR: Step 1, formation of charge-transfer complex with NADH; step 2, flavin reduction by NADH; step 3, release of NAD^+ from two electron-reduced MR; step 4, formation of charge-transfer complex with codeinone; step 5, electron transfer from MR to codeinone; step 6, release of hydrocodone and regeneration of unliganded oxidized MR.

by the simplified scheme described previously for OYE, but the slow electron-transfer rates observed for MR with this substrate prevented analysis of this reaction by sequential stopped-flow methods in the presence of molecular oxygen.

The reaction-catalyzed MR can be summarized by the kinetic scheme shown in Figure 9. Our kinetic work did not provide a means of directly measuring the rate of NAD^+ release from reduced enzyme at the completion of the reductive half-reaction, but the process is clearly complete before initiation of the oxidative half-reaction using the sequential mixing stopped-flow method. Reduction of the flavin by NADH is reversible, since reduction of the enzyme with stoichiometric, or greater than stoichiometric (e.g., 5 × molar excess), amounts of NADH did not effect complete reduction to the dihydroflavin form. In reductive reactions performed with excess NADH (e.g., 100 × molar excess), reduction of the flavin was effectively complete. Attempts were made to measure the rate of NAD^+ reduction by reduced enzyme by using a variation of the sequential mixing protocol described for the oxidative half-reaction with codeinone. In this case, enzyme was prereduced with a stoichiometric concentration of NADH, and following a suitable delay (700 ms), the reduced enzyme was mixed with NAD^+ (at concentrations up to 25 mM). Analysis of these reactions by multiple wavelength spectroscopy using the photodiode array revealed that reoxidation of the flavin was mediated by molecular oxygen rather than by electron transfer to NAD^+: no large spectral changes at 340 (indicative of the production of NADH) or at 550 nm (charge-transfer complex formation) were observed, but reoxidation of the flavin was observed at 462 nm. The data reveal that the rate of reduction of NAD^+ by reduced enzyme is slower than the intrinsic oxidase rate (about 0.2 s^{-1}) of MR.

The thermodynamic parameters calculated for the reductive half-reaction of MR have enabled a partial energy profile for MR to be constructed. Unfortunately, due to the prohibitive amounts of codeinone required, the thermodynamic analyses could not be extended to the oxidative half-reaction. Notwithstanding, the changes in entropy, enthalpy, and Gibbs free energy for both transition states in the reductive half-reaction are consistent with what is known concerning the chemistry of flavin and the reaction sequence of MR. For example, during electron transfer to the flavin, negative charge will develop in the region of the N1 atom and C2 carbonyl group of the flavin and a positive charge will be formed on the nicotinamide cofactor. These charge developments are consistent with the large negative entropy

change associated with electron transfer, and will reflect (among other things) the ordering of solvent molecules around these charges. In comparison, the change in entropy for the charge-transfer step was found to be weakly negative. This is a result mainly of combined contributions from immobilization of NADH (negative entropy change) on the enzyme and desolvation of the active site (positive entropy change), and perhaps suggests that the latter process is important in MR. Indeed, the crystallographic structure of MR indicates that the active site is solvent-exposed and is therefore most likely bathed in solvent molecules in the nonliganded form.

The kinetic parameters determined for the oxidative half-reaction of MR indicate that this part of the reaction pathway is far from optimal. The dissociation constant for codeinone (closely related to morphinone; see Figure 1) indicates relatively poor binding of this substrate by the enzyme. This in part is due to the small second-order rate constant for formation of the charge-transfer complex. The rates for electron transfer to codeinone (about 45 s^{-1}), and in particular the release of the product hydrocodone from oxidized enzyme (about 2.5 s^{-1}), are poor. These findings are no doubt a reflection on the late evolution of MR from an ancestral Class I flavin-dependent β/α barrel oxidoreductase, since the producing organism was isolated from industrial waste liquors derived from an opiate-producing factory (*1*). The detailed kinetic and thermodynamic analysis of wild-type MR coupled with the recent determination of the crystallographic structure for the enzyme have substantially furthered our understanding of catalysis by this biotechnologically important enzyme. On the longer term, it is hoped that it will also contribute to our understanding of the evolution of the Class I flavin-dependent β/α barrel oxidoreductase family.

ACKNOWLEDGMENTS

We thank MacFarlan Smith Ltd for the supply of codeinone (on a gratis basis) and Professor S. Ghisla (University of Konstanz) for kindly supplying 5-deazaflavin mononucleotide. We also thank Applied Photophysics and Belle Technology Ltd for technical assistance in developing anaerobic stopped-flow facilities at Leicester University. We also gratefully acknowledge Dr. K. Lilley (University of Leicester) for performing MALDI-TOF mass spectrometry analysis of codeinone.

REFERENCES

1. Bruce, N. C., Wilmot, C. J., Jordan, K. N., Trebilcock, A. E., Gray Stephens, L. D., and Lowe, C. R. (1990) *Arch. Microbiol. 154*, 465−470.
2. Melmon, K. L., and Morrelli, H. F. (1972) *Clinical pharmacology: basic principles in therapeutics*, Macmillan Publishing Co., New York.
3. Moffat, A. C., Jackson, J. V., Moss, M. S., and Widdop, B. (1986) *Clarke's isolation and identification of drugs*, The Pharmaceutical Press, London.
4. Bruce, N. C., French, C. E., Hailes, A. M., Long, M. T., and Rathbone, D. A. (1995) *Trends Biotechnol. 13*, 200−205.
5. Willey, D. L., Caswell, D. A., Lowe, C. R., and Bruce, N. C. (1993) *Biochem. J. 290*, 539−544.
6. French, C. E., Hailes, A. M., Rathbone, D. A., Long, M., Willey, D. L., and Bruce, N. C. (1995) *Bio/Technology 13*, 674−676.
7. French, C. E., and Bruce, N. C. (1995) *Biochem. J. 312*, 671−678.
8. Scrutton, N. S. (1994) *BioEssays 16*, 115−122.
9. Stott, K., Saito, K., Thiele, D. J., and Massey, V. (1993) *J. Biol. Chem. 268*, 6097−6106.
10. French, C. E., Nicklin, S., and Bruce, N. C. (1996) *J. Bacteriol. 178*, 6623−6627.
11. Snape, J. R., Walkley, N. A., Morby, A. P., Nicklen, S., and White, G. F. (1997) *J. Bacteriol. 179*, 7796−7802.
12. Madani, N. D., Malloy, P. J., Rodriguez-Pombo, P., Krishan, A. V., and Feldman, D. (1994) *Proc. Natl. Acad. Sci. U.S.A. 91*, 922−926.
13. Boyd, G., Mathews, F. S., Packman, L. C., and Scrutton, N. S. (1992) *FEBS Lett. 308*, 271−276.
14. Yang, C.-C., Packman, L. C., and Scrutton, N. S. (1995) *Eur. J. Biochem. 232*, 264−271.
15. Liu, X. L., and Scopes, R. (1993) *Biochim. Biophys. Acta 1174*, 187−190.
16. Mallonee, D. H., White, W. B., and Hylemon, P. B. (1990) *J. Bacteriol. 172*, 7011−7019.
17. Franklund, C. V., Baron, S. F., and Hylemon, P. B. (1993) *J. Bacteriol. 175*, 3002−3012.
18. Moody, P. C. E., Shikotra, N., French, C. E., Bruce, N. C., and Scrutton, N. S. (1997) *Acta Crystallogr. D53*, 619−621.
19. Raine, A. R. C., Scrutton, N. S., and Mathews, F. S. (1994) *Protein Sci. 3*, 1889−1892.
20. Fox, K. M., and Karplus, P. A. (1994) *Structure 2*, 1089−1105.
21. French, C. E., and Bruce, N. C. (1994) *Biochem. J. 301*, 97−103.
22. Sambrook, J., Fritsch, E. F., and Maniatis, T. (1989) *Molecular cloning: a laboratory manual*, 2nd ed., Cold Spring Harbor Laboratory Press, Cold Spring Harbor, NY.
23. Massey, V., and Palmer, G. (1966) *Biochemistry 5*, 3181−3189.
24. Massey, V., Stankovich, M., and Hemmerich, P. (1978) *Biochemistry 17*, 1−8.
25. Massey, V., and Hemmerich, P. (1978) *Biochemistry 17*, 9−17.
26. Leatherbarrow, R. J. (1990) Grafit version 2.0, Erithacus Software Ltd., Staines, U.K.
27. Narlikar, G. J., and Herschlag, D. (1996) *Nat. Struct. Biol. 3*, 701−710.
28. Massey, V., and Schopfer, L. M. (1986) *J. Biol. Chem. 261*, 1215−1222.

BI980345I